Modeling Hysteresis and Its Inverse Model Using Neural Networks Based on Expanded Input Space Method

Xinlong Zhao and Yonghong Tan

***Abstract*—A neural network-based approach of identification for hysteresis and its inverse model is proposed. In this method, a hysteretic operator is proposed to extract the change tendency of hysteresis. Then, an expanded input space is constructed to transform the multivalued mapping into one-to-one mapping so that the neural networks are capable of implementing identification for hysteresis. Similar to the method of modeling hystereis, an inverse hyteretic operator is proposed to construct an inverse model for hysteresis. Then the experimental results are presented to illustrate the potential of the proposed modeling technique.**

***Index Terms*—Hysteresis, hysteretic operator, inverse model, modeling, neural networks.**

I. Introduction

PIEZOELECTRIC actuators are widely used in micro-positioning and ultra-precision manufacturing systems. However, one of the drawbacks of the piezoelectric actuator is the existence of hysteresis. Hysteresis is a multi-valued mapping and is non-differentiable, thus it presents a challenge in the control of systems with piezoelectric actuators. Without modeling and incorporating hysteresis in the controller design, hysteresis often severely limits system performance such as giving rise to undesirable inaccuracies or oscillations, even leading to instability [1]. Therefore, it is necessary to find a model describing the behavior of hysteresis so that the corresponding controller based on the obtained hysteresis model can be designed to eliminate the harmful effect of hysteresis. In recent decades, there have been several models proposed to describe the hysteresis, such as the Preisach model [2], [3], the KP hysteron model [4], the PI model [5], and the Bouc–Wen model [6]. Among those models, the Preisach model is the most popular one since it contains the basic features of the hysteresis phenomena in a conceptually simple and mathematically elegant way. It has been widely used to model some smart materials such as ferromagnet, piezoceramic, and shape-memory alloy. However, it is not convenient to tune the parameters online in order to adapt to the change of operating environment. Moreover, another drawback of the Preisach model is that it is not easy to determine the values of the distribution function of the model.

Manuscript received December 20, 2005; revised January 21, 2007. Manuscript received in final form May 23, 2007. Recommended by Associate Editor C.-Y. Su. This work was supported in part by the National Science Foundation of China under Grant 60572055 and by the Guangxi Science Foundation under Grant 0339068.

X. Zhao is with Institute of Automation, Zhejiang Sci-Tech University, Hangzhou 310018, China (e-mail: zhaoxinlong@hotmail.com).

Y. Tan is with the School of Electronic Engineering, University of Electronic Science and Technology of China, Chengdu 610054, China (e-mail: tany@guet.edu.cn).

Color versions of one or more of the figures in this paper are available online at http://ieeexplore.ieee.org.

Digital Object Identifier 10.1109/TCST.2007.906274

Recently, artificial neural networks have been applied to modeling of hysteresis. Adly and Abd-El-Hafiz [7] had proposed a neural model. In their method, the Presach model was considered as the superposition of the outputs of a set of elementary hysteresis operators. Then the weights function of those operators were determined by neural networks. Serpico and Visone [8] also proposed a feedforward neural network-based hysteresis model. This neural model was composed of two blocks. The first one was a block with memory that was constituted by a set of play operators. The second one was a memoryless function approximated by a feedforward neural network. The above-mentioned neural network-based methods are useful for modeling hysteresis. However, the drawbacks still exist, such as the fact that the procedure of realization is rather complicated. Li and Tan [9] also proposed a neural networks model for hysteresis. In their method, a hysteretic operator motivated by the Preisach model was defined to decompose the multivalued mapping of hysteresis into a one-to-one mapping between the input coordinates and the output so that the neural networks can be utilized for model approximation. The disadvantage of the method was that the hysteretic operator used to extract the boundary of the integral area was still complicated in engineering practice.

In order to control systems with hysteresis, the most common approach is to construct an inverse model of hysteresis. Gang Tao and Kokotovic [1] presented a simple parameterized hysteresis model and developed a corresponding inverse model for it. As the parameterized hyteresis model could not describe the real hysteresis accurately, the derived inverse model would result in large error. Webb [10] also proposed a linearly parameterized KP model as well as the inverse model based on the obtained KP model. However, the process of deriving its precise inverse model is complicated.

In this paper, a novel hysteretic operator is proposed to construct an expanded input space so as to transform the multivalued mapping of hysteresis into a one-to-one mapping which enables neural networks to approximate the behavior of hysteresis.

In some cases, for instance, in the design procedure of internal model control strategy, it requires the development of both the model and the inverse model. As hysteresis is a nonsmooth nonlinear function with multivalued mapping, it is rather difficult to derive an inverse model directly based on the obtained hysteretic model based on the proposed hysteretic operator. Therefore, a new operator is proposed in order to construct an inverse model describing the inverse behavior of hysteresis. Similar to the procedure of construction for a hysteretic operator, an inverse hysteretic operator is proposed. Then, a neural network-based inverse model for hysteresis is developed. The obtained expanded input space is proved to be compact. Moreover, the proof of the continuity of the one-to-one mapping is presented. Comparing

with the previous-stated methods, the proposed transformation operators can extract the variation tendency of the hysteresis or inverse hysteresis. Then, a new input space is constructed by introducing additional coordinates into the input space. The introduced additional coordinates are actually determined by the proposed transformation operators. Thus, the output of the hysteresis or the inverse hysteresis can be uniquely specified by the constructed expanded input space. Furthermore, the proposed transformation operators can be easily determined, and the neural network-based hysteresis or inverse hysteresis model has a rather simple architecture.

II. Hysteretic Operator

Recently, artificial neural networks have been widely applied to pattern recognition and system identification. However, it is known that neural networks can only be available for the approximation of the continuous systems with one-to-one or multiple-to-one mappings. It is unable to use the traditional techniques of system identification as well as the neural networks to directly identify the model of systems with multivalued mapping such as hysteresis [11]. In order to handle this problem, a transformation operator is proposed to extract the variation feature of the hysteresis. Then, in terms of the proposed transformation operator, an expanded input space is constructed to transform the multivalued mapping of hysteresis into a one-to-one mapping.

The proposed hysteretic operator $h(x)$ is defined as

$$h(x) = \left(1 - e^{-|x-x_p|}\right)(x - x_p) + h(x_p) \tag{1}$$

where x is the current input, $h(x)$ is the current output, and x_p is the dominant extremum adjacent to the current input x. $h(x_p)$ is the output of the operator when the input is x_p.

Assumption 1: The considered hysteresis is continuous and forms a closed loop in the input–output diagram when the input cycles between two extrema.

Lemma 1: Let $x(t) \in C(R^+)$, where $R^+ = \{t | t \geq 0\}$ and $C(R^+)$ is the set of continuous functions on R^+. For the different time instances t_1 and t_2, it results in $t_1 \neq t_2$, but $x(t_1) = x(t_2)$, where $x(t_1)$ and $x(t_2)$ belong to an ascending curve and a descending curve, respectively. The ascending curve and the descending curve are connected by a point corresponding to an extremum. Then, this leads to $h[x(t_1)] \neq h[x(t_2)]$.

Proof: Considering that the segment $x(t)$ decreases monotonically, (1) becomes

$$h(x) = h_{de}(x) = (1 - e^{x-x_p})(x - x_p) + h(x_p), \quad \dot{x}(t) < 0 \tag{2}$$

where $h_{de}(x)$ is the decreasing segment of the function and x_p is the maximum extremum of the input, while

$$h(x) = h_{\text{in}}(x) = \left[1 - e^{-(x-x_p)}\right](x - x_p) + h(x_p), \quad \dot{x}(t) > 0 \tag{3}$$

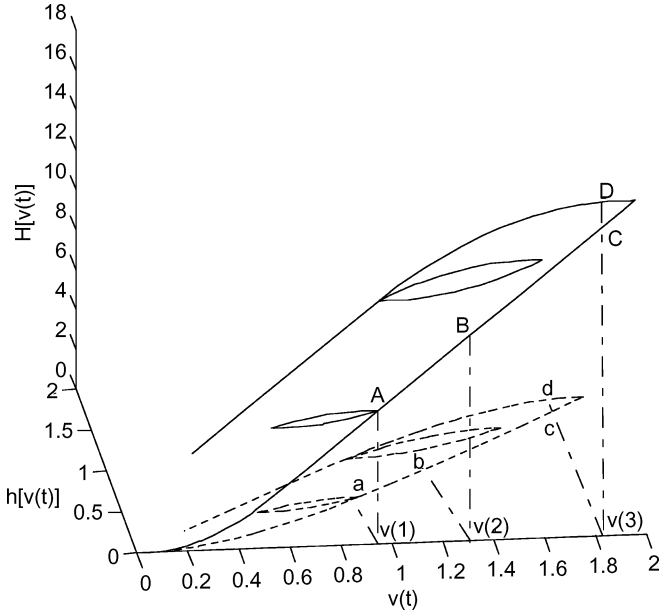

Fig. 1. Behavior of the hysteretic operator.

denotes the increasing segment of the function. In this case, x_p is the minimum extremum of the input. Since

$$\begin{aligned} \frac{dh_{\text{in}}(x)}{dx} &= e^{-(x-x_p)} \cdot (x - x_p) + \left[1 - e^{-(x-x_p)}\right] \\ &= 1 - \frac{1 - (x - x_p)}{e^{x-x_p}} > 1 - \frac{1}{e^{x-x_p}} > 0 \end{aligned} \tag{4}$$

then $h_{\text{in}}(x)$ is monotonic. Similarly, one can obtain that $h_{de}(x)$ is also monotonic.

It is noticed that $h_{\text{in}}(x)$ is obtained from $h_{in0}(x) = (1 - e^{-x})x$ $(x \geq 0)$. Its origin moves from (0,0) to $(x_p, h(x_p))$. On the other hand, $h_{de}(x)$ is obtained from $h_{de0}(x) = (1 - e^{x})x$ $(x \leq 0)$ when its origin moves from (0,0) to $(x_p, h(x_p))$. Since $h_{in0}(-x) = -h_{de0}(x)$, it implies that $h_{\text{in}}(x)$ and $h_{de}(x)$ are antisymmetrical functions. Thus, it can be concluded that $h_{\text{in}}(x)$ and $h_{de}(x)$ intersect only at extremum point $(x_p, f(x_p))$, that is, if $x(t_1)$ and $x(t_2)$ are not the extrema, but $x(t_1) = x(t_2)$, then

$$h\left[x(t_1)\right] \neq h\left[x(t_2)\right].$$

Remark 1: Suppose $H[\cdot]$ is defined as the output of hysteresis. When $h[\cdot]$ and $H[\cdot]$ are fed with the same input $v(t)$, the curve of $h[v(t)]$ exhibits behavior similar to that of $H[v(t)]$ such as ascending, turning, and descending.

In the following, an example is provided to illustrate this similarity. Suppose a hysteresis constructed by ten backlash operators with the values of the deadband width evenly distributed within (0.1,1). The input fed into the hysteresis is $v(t) = 1.5\sin(0.5t) + 0.5\sin(3t)$. The curve of hysteresis (solid) and that of the corresponding hysteretic operator (dashed line) are shown in Fig. 1. It is obvious that the hysteresis exhibits nonsmooth behavior and multivalued mapping.

From Fig. 1, when $v(1)$ is fed into $h(v)$ and $H(v)$, the corresponding outputs of $h(v)$ and $H(v)$ are respectively points a and A. For input $v(2)$, the resulted outputs of $h(v)$ and $H(v)$

are, respectively, points b and B. It can be seen that the proposed hysteretic operator can extract the main feature of the hysteresis if it is fed with the same input as that of the hysteresis. The curve of hysteresis is very similar to that of hysteretic operator.

Remark 2: As $v(t_1) = v(t_2)$, where $v(t_1)$ and $v(t_2)$ belong to an ascending curve and a descending curve, respectively, and $h[v(t_1)] \neq h[v(t_2)]$, then the coordinate $(v(t), h[v(t)])$ is uniquely corresponding to the output of hysteresis $H[v(t)]$.

Lemma 2: If there exist two time instances t_1 and t_2, also $t_1 \neq t_2$, and $x(t_1)$ and $x(t_2)$ belong to an ascending curve or a descending curve, such that $h[x(t_1)] - h[x(t_2)] \to 0$, then $x(t_1) - x(t_2) \to 0$.

Proof: Assume that the segment $x(t)$ increases monotonically. From the proof of Lemma 1, it follows that

$$h_{\text{in}}(x) = \left[1 - e^{-(x-x_p)}\right](x - x_p) + h(x_p)$$

is monotonic as

$$x(t_1) - x(t_2) \to 0 \Rightarrow h_{\text{in}}[x(t_1)] - h_{\text{in}}[x(t_2)] \to 0. \quad (5)$$

According to the property of continuity of the inverse function, it yields

$$h_{\text{in}}[x(t_1)] - h_{\text{in}}[x(t_2)] \to 0 \Rightarrow x(t_1) - x(t_2) \to 0. \quad (6)$$

Similar to h_{in}, this results in

$$h_{de}[x(t_1)] - h_{de}[x(t_2)] \to 0 \Rightarrow x(t_1) - x(t_2) \to 0. \quad (7)$$

Then, it can be obtained that

$$h[x(t_1)] - h[x(t_2)] \to 0 \Rightarrow x(t_1) - x(t_2) \to 0. \quad (8)$$

Theorem 1: For any hysteresis satisfying Assumption 1, there exists a continuous one-to-one mapping $\Gamma : R^2 \to R$, such that $H[v(t)] = \Gamma(v(t), h[v(t)])$.

Proof: First, it is proved that Γ is a one-to-one mapping.

Situation 1: Assume that $v(t)$ is not the extremum.

In terms of Lemma 1, for two different time instances t_1 and t_2, $v(t_1) = v(t_2)$; if $v(t_1)$ and $v(t_2)$ belong to an ascending curve and a descending curve, respectively, then

$$(v(t_1), h[v(t_1)]) \neq (v(t_2), h[v(t_2)]).$$

If $v(t_1)$ and $v(t_2)$ locate at different ascending curves or different descending curves with different dominant extremum, $h[v(t_1)]$ and $h[v(t_2)]$ can only intersect at an extremum. It can be obtained that

$$(v(t_1), h[v(t_1)]) \neq (v(t_2), h[v(t_2)]).$$

Therefore, the coordinate, i.e., $(v(t), h[v(t)])$, is uniquely corresponding to hysteresis $H[v(t)]$.

Situation 2: Suppose that $v(t)$ is the extremum.

In this case, for two different time instances t_1 and t_2, there will be

$$(v(t_1), h[v(t_1)]) = (v(t_2), h[v(t_2)]).$$

Because $v(t)$ is the extremum, then $H[v(t_1)] = H[v(t_2)]$. Also, coordinate $(v(t), h[v(t)])$ is uniquely corresponding to hysteresis $H[v(t)]$.

Combining the above-mentioned two situations, it is obtained that Γ is a one-to-one mapping. Next, it will be verified that Γ is a continuous mapping.

According to the property of hysteresis curve

$$v(t_1) - v(t_2) \to 0 \quad \Rightarrow H[v(t_1)] - H[v(t_2)] \to 0. \quad (9)$$

Then, considering lemma 2, we have

$$h[v(t_1)] - h[v(t_2)] \to 0 \Rightarrow v(t_1) - v(t_2) \to 0 \Rightarrow H[v(t_1)] - H[v(t_2)] \to 0. \quad (10)$$

Therefore, it can be concluded that there exists a continuous one-to-one mapping $\Gamma : R^2 \to R$ such that $H[v(t)] = \Gamma(v(t), h[v(t)])$.

Remark 3: The straightforward explanation of Theorem 1 can be illustrated in Fig. 1. It can further be found out that $H(v)$ can uniquely be determined by the point in the $v - h(v)$-plane. Assuming that $v(t_1) = v(t_2) = v(3)$ for two different time instances t_1 and t_2, the corresponding outputs of $H(v)$ are, respectively, $H[v(t_1)]$ (point C in Fig. 1) and $H[v(t_2)]$ (point D in Fig. 1); moreover, $H[v(t_1)] \neq H[v(t_2)]$. The phenomena that happened are due to the multivalued characteristic of hysteresis. Considering the introduced operator, i.e., $h(v)$, for $v(t_1) = v(t_2) = v(3)$, the resulted outputs of $h(v)$ are $h[v(t_1)] \neq h[v(t_2)]$, where $h[v(t_1)]$ corresponds to point c and $h[v(t_2)]$ to point d in Fig. 1. Therefore, based on point $(v(t_1), h[v(t_1)])$ in the $v - h(v)$-plane through mapping Γ, it can uniquely determine $H[v(t_1)]$. Moreover, point $(v(t_2), h[v(t_2)])$ in the $v - h(v)$-plane through mapping Γ, it can also uniquely determine $H[v(t_2)]$.

III. Inverse Hysteretic Operator

As the previous discussion stated, in some cases, for instance, in the design procedure of internal model control strategy, it requires to construct both the model and the inverse model. However, it is known that hysteresis is a nonsmooth nonlinear function with multivalued mapping, it is rather difficult to obtain an inverse model directly based on the obtained hysteretic model based on the proposed hysteretic operator. Hence, similar to the method of the construction of a transformation operator for modeling of hysteresis, an inverse hysteretic operator is proposed to transform the multivalued mapping of the inverse mapping of hysteresis into one-to-one mapping. The proposed inverse hysteretic operator is defined as

$$h_{\text{inv}}(x) = \ln\left(\sqrt{(x - x_p)^2 + 1} + (x - x_p)\right) + h_{\text{inv}}(x_p) \quad (11)$$

where x is the current input, $h_{\text{inv}}(x)$ is the current output, x_p is the dominant extremum adjacent to the current input, and $h_{\text{inv}}(x_p)$ is the output of the inverse hysteretic operator when the input is x_p.

Remark 4: It is assumed that $H_{\text{inv}}[\cdot]$ is defined as the output of the inverse hysteresis. When $h_{\text{inv}}[\cdot]$ and $H_{\text{inv}}[\cdot]$ are fed with

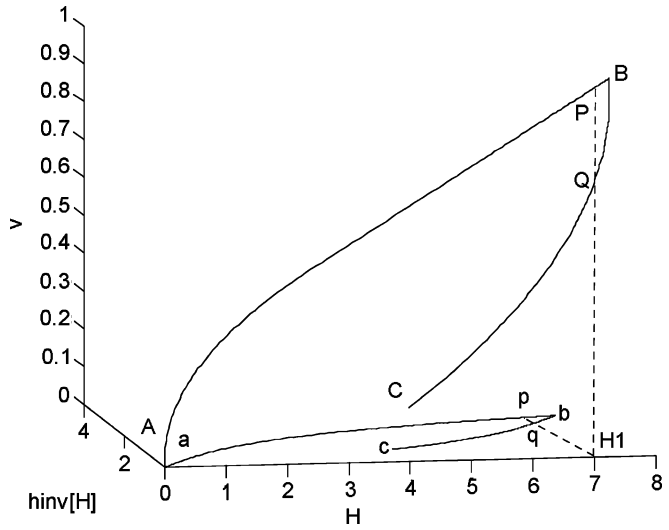

Fig. 2. Behavior of the inverse hysteretic operator.

the same input $u(t)$, the curve of $h_{\text{inv}}[u(t)]$ exhibits the similarity to that of $H_{\text{inv}}[u(t)]$ such as ascending, turning, and descending. There is only a little difference between $h_{\text{inv}}(x)$ and $h(x)$. With the change of input, the rotation of the loop of hysteretic operator $h(x)$ is in the counterclockwise direction, while the rotation of the loop of inverse hysteretic operator $h_{\text{inv}}(x)$ is in the clockwise direction.

Remark 5: $h_{\text{inv\_in}}(x)$ denotes the increasing segment of the function. On the other hand, $h_{\text{inv\_de}}(x)$ denotes the decrease segment of the function. It is noticed that $h_{\text{inv\_in}}(x)$ is obtained from $h_{\text{inv0}}(x) = \ln(\sqrt{x^2+1}+x)(x \geq 0)$. Its origin moves from (0,0) to $(x_p, h(x_p))$. On the other hand, $h_{\text{inv\_de}}(x)$ is obtained from $h_{\text{inv0}}(x) = \ln(\sqrt{x^2+1}+x)$ $(x \leq 0)$ when its origin moves from (0,0) to $(x_p, h(x_p))$. Since $h_{\text{inv0}}(-x) = -h_{\text{inv0}}(x)$, the inverse hysteretic operator, i.e., $h_{\text{inv}}(x)$ can be decomposed into an ascending curve function $h_{\text{inv\_in}}(x)$ and a descending curve function $h_{inv\_de}(x)$. Moreover, $h_{\text{inv\_in}}(x)$ and $h_{\text{inv\_de}}(x)$ are antisymmetrical functions.

Similar to the proof of Theorem 1, the corresponding Theorem 2 is shown in the following.

Theorem 2: For any inverse hysteresis, $u(t)$ and $H_{\text{inv}}[u(t)]$ are respectively defined as the input and output of the inverse hysteresis, and there exists a continuous one-to-one mapping $\Psi : R^2 \to R$ such that $H_{\text{inv}}[u(t)] = \Psi(u(t), h_{\text{inv}}[u(t)])$.

The procedure of the proof of Theorem 2 is similar to that of Theorem 1, so it is omitted due to the limitation of space. Moreover, Fig. 2 illustrates the behavior of the inverse hysteretic operator and the straightforward explanation of Theorem 2.

IV. Neural Network-Based Identification for Both Hysteresis and Inverse Hystereisis

Theorem 1 indicates that the multivalued mapping of hysteresis can be transformed into a one-to-one mapping based on the proposed expanded input space containing the transformation operator. It is also proved that the obtained mapping is a continuous mapping.

Let $T = [t_0, \infty) \in R$, $V = \{v | T \xrightarrow{v} R\}$, and $F = \{h | T \xrightarrow{h} R\}$ be the input sets. Given $t_i \in T$, it is obvious that $v(t_i) < +\infty$ and $h[v(t_i)] < +\infty$, thus $(v(t_i), h[v(t_i)]) \in R^2$. It can been seen that the constructed input space, i.e., $\Phi = \{(v(t_i), h[v(t_i)]) | v(t_i) \in V, h[v(t_i)] \in F\}$ is a compact set.

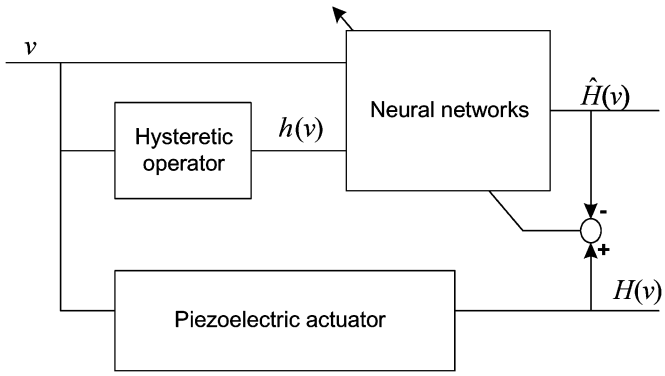

Fig. 3. Schematic diagram of neural networks-based hysteresis model.

Based on what was stated above, the neural networks can be now applied to the modeling of the hysteresis since the hysteresis transformation operator is introduced to construct a coordinate in order to realize the decomposition of multi-valued mapping of hysteresis into a one-to-one mapping. It is known that multilayer feedforward neural networks (MFNN) are capable of approximating any continuous function on a compact set in arbitrary accuracy. Therefore, the MFNN used to identify the hysteresis is shown as follows:

$$\Gamma(v(t), h[v(t)]) = NN(v(t), h[v(t)]) + \varepsilon$$

where $NN(\cdot)$ represents MFNNs. ε is the approximation error, for any $\varepsilon_N > 0$, $|\varepsilon| \leq \varepsilon_N$.

The schematic diagram of neural networks-based hysteresis model is shown in Fig. 3.

Similar to the procedure of modeling hysteresis, some conclusions about the modeling of inverse hysteresis are also derived.

Theorem 2 also indicates that the multivalued mapping of the inverse hysteresis can be transformed into a one-to-one mapping based on the proposed expanded input space containing the proposed inverse hysteretic operator. Similar to the proof of the continuity of the hysteresis mapping, it is also derived that the inverse hysteresis mapping can also be proved to be a continuous mapping.

Let $T = [t_0, \infty) \in R$, $U = \{u | T \xrightarrow{u} R\}$, and $P = \{h_{\text{inv}} | T \xrightarrow{h_{\text{inv}}} R\}$ be the input sets. Given $t_i \in T$, it is obvious that $u(t_i) < +\infty$ and $h[u(t_i)] < +\infty$, thus $(u(t_i), h_{\text{inv}}[u(t_i)]) \in R^2$. It can be seen that $\Theta = \{(u(t_i), h_{\text{inv}}[u(t_i)]) | u(t_i) \in U, h_{\text{inv}}[u(t_i)] \in P\}$ is also a compact set.

Therefore, the MFNNs used to identify the inverse hysteresis is shown as follows:

$$\Psi(u(t), h_{\text{inv}}[u(t)]) = NN(u(t), h_{\text{inv}}[u(t)]) + \varepsilon$$

where $NN(\cdot)$ represents MFNNs. ε is the approximation error, for any $\varepsilon_N > 0$, $|\varepsilon| \leq \varepsilon_N$.

Fig. 4. Piezoelectric actuator (PZT-753.21C).

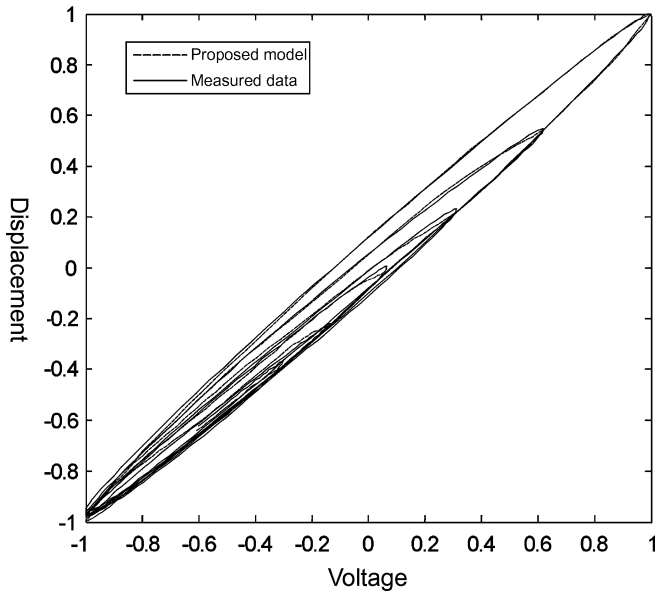

Fig. 5. Validation result of the proposed model.

V. Experimental Results

A. Hysteresis model

Here, the proposed approach is applied to the identification of the hysteresis in a piezoelectric actuator (PZT-753.21C) shown in Fig. 4. The comparison of the performance between the obtained neural model and the KP model is also presented.

The actuator has a nominal expansion of 0–25 μm under the input voltage within 0–100 V. In this experiment, it is excited with 5-Hz exponential decayed sinusoidal voltages. The sampling frequency is 1000 Hz. After filtering, 1200 pairs of samples are selected to construct the training set and normalized so that the data set is located within $[-1,1]$.

The architecture of the neural model consists of two input nodes, twelve hidden neurons, and one output neuron. The input of the neural model is $(v(t), h[v(t)])$. The sigmoid and linear functions are respectively used as the activation function in the hidden layer and in the output layer. In this experiment, the conjugate gradient algorithm with the Powell–Beale restarted method [12] is used to train the neural networks so as to improve the convergent rate and the performance of the neural model. This algorithm is distinguished with two features. First, the algorithm uses a test to determine when to reset the search direction to the negative of the gradient. Second, the search direction

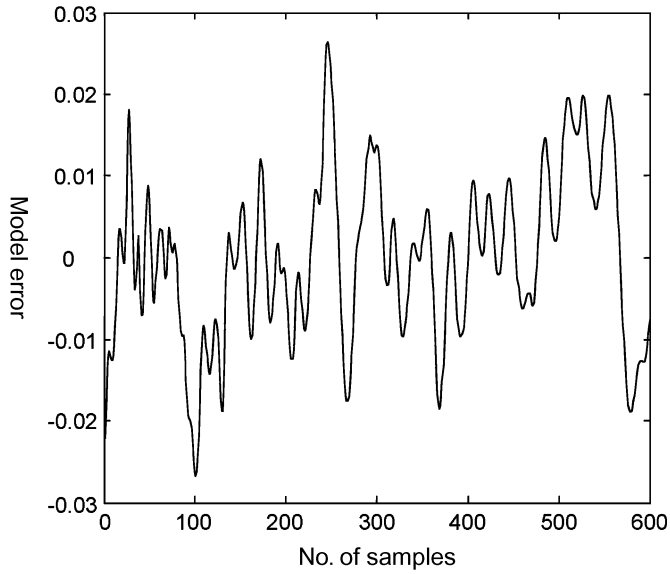

Fig. 6. Validation error of the proposed model.

is computed from the negative gradient, the previous search direction, and the last search direction before the previous reset. The data used for experiment are separated into two parts. One part is used for model identification and the other part is used for model validation. With 463 epochs, the training procedure is finished. Fig. 5 shows the result of model validation. Fig. 6 demonstrates the model validation error. The maximum error is 0.026735. The mean square error is 0.01027. The first-to-second lay interconnection weight matrices in modeling hysteresis is

$$V^T = \begin{bmatrix} 0.92868 & -4.2834 \\ 2.9751 & -3.4106 \\ 2.8525 & 2.6649 \\ 4.1082 & -2.0442 \\ -4.4328 & 1.1746 \\ 2.4104 & -3.7905 \\ -2.8838 & 3.9424 \\ 3.6841 & -2.2516 \\ -0.1280 & 4.5199 \\ 2.4722 & 4.3035 \\ -2.9421 & 3.8524 \\ -4.6679 & -0.0671 \end{bmatrix}.$$

The second-to-third lay interconnection weight matrices in modeling hysteresis becomes

$$\begin{aligned} \mathrm{W^T} = [&0.14746\ 0.19485\ 0.18544\ 0.29217\ -0.063771 \\ &-0.23641\ 0.36609\ 0.38883\ 0.062557 \\ &-0.010069\ -0.22648\ -0.13171]. \end{aligned}$$

The model validation result of the KP model [10] and the model validation error are respectively shown in Figs. 7 and 8. The KP model consists of 210 KP operators. The derived maximum error of the model is 0.0363 and the mean square error is 0.013.

Compared with the KP model, the proposed neural model has a simple architecture and a simplified identification procedure.

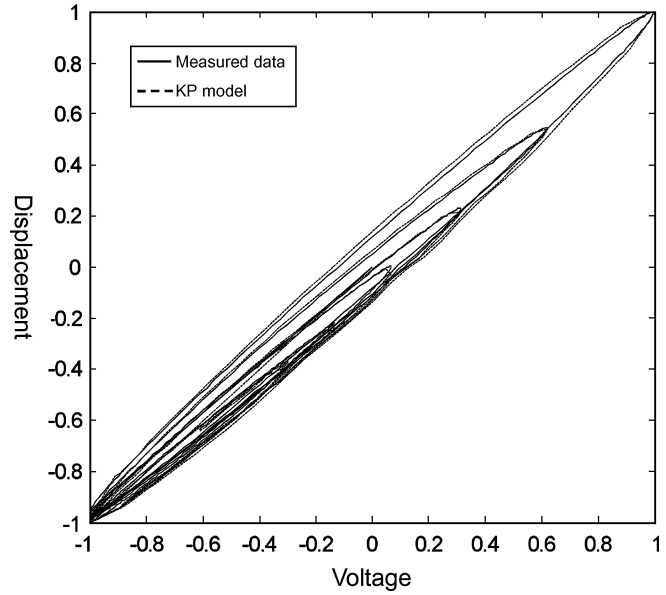

Fig. 7. Validation result of the KP model.

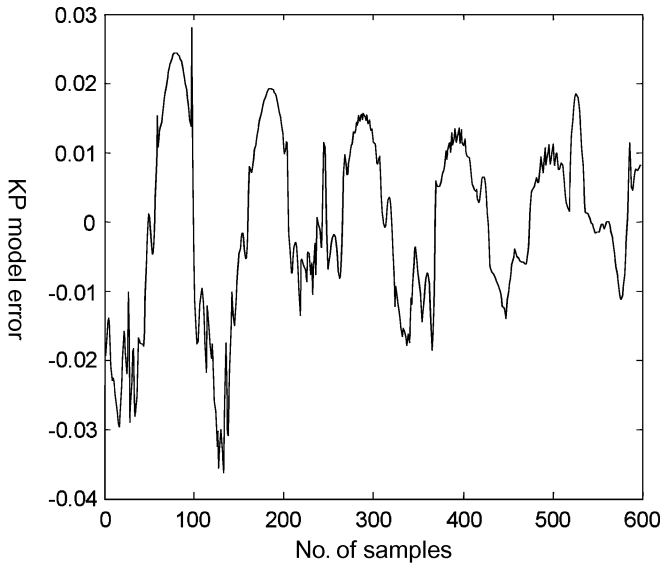

Fig. 8. Validation error of the KP model.

B. Inverse Hysteresis Model

The architecture of the neural inverse model consists of two input nodes, twelve hidden neurons, and one output neuron. The sigmoid and linear functions are respectively used as the activation functions in the hidden layer and in the output layer. Then, the conjugate gradient algorithm with the Powell–Beale restarted method [12] is used to train the neural networks. The obtained inverse hysteresis model as well as the model validation error are respectively shown in Figs. 9 and 10.

The first-to-second lay interconnection weight matrices in modeling inverse hysteresis is

$$\begin{aligned}\mathrm{V}^{\mathrm{T}} = [&0.66911\ -7.3496;\ -3.8476\ -5.4962;\ 3.9844\\ &4.9896;\ 4.6378\ -3.4216;\ -5.5681\ 0.71356;\\ &3.2721\ -6.7838;\ -3.4185\ 5.4921;\ 5.334\\ &-3.157;\ 0.40291\ 7.2651;\ 2.3698\ 6.3681;\\ &-3.4173\ 5.8441;\ -6.0485\ -0.14439].\end{aligned}$$

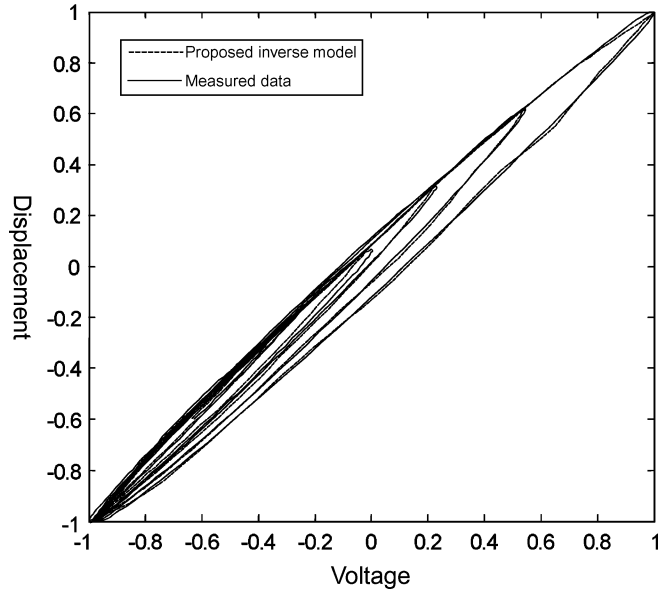

Fig. 9. Validation result of the proposed inverse model.

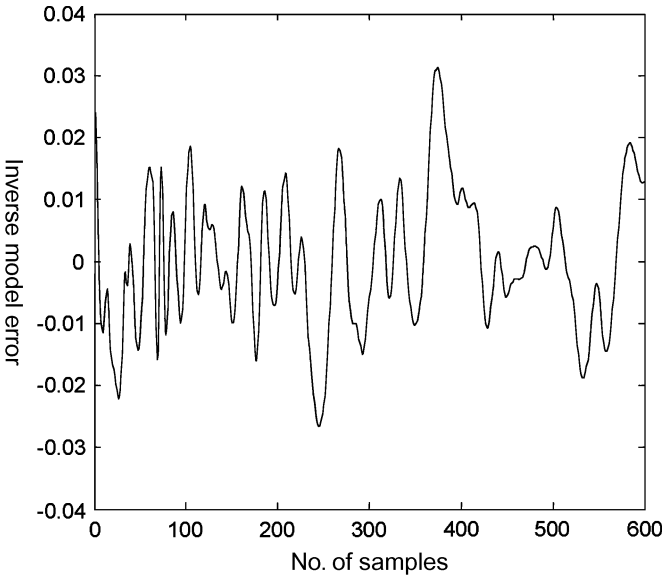

Fig. 10. Validation error of the proposed inverse model.

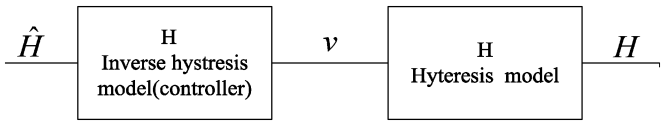

Fig. 11. Piezoelectric actuator linearization with inverse hysteresis model.

The second-to-third lay interconnection weight matrices in modeling inverse hysteresis is

$$\begin{aligned}\mathrm{W}^{\mathrm{T}} = [&-0.28204\ 0.11689\ 0.14338\ 0.32046\ -0.11074\\ &-0.18919\ 0.44428\ 0.20197\ 0.039379\ 0.042013\\ &-0.56074\ -0.037487].\end{aligned}$$

In order to eliminate the effect of hysteresis, one of the most popular methods is to construct an inverse hysteresis model to be in cascade with the hysteresis. The corresponding system architecture is shown in Fig. 11. In this architecture, the proposed neural network-based inverse hysteresis model is used as

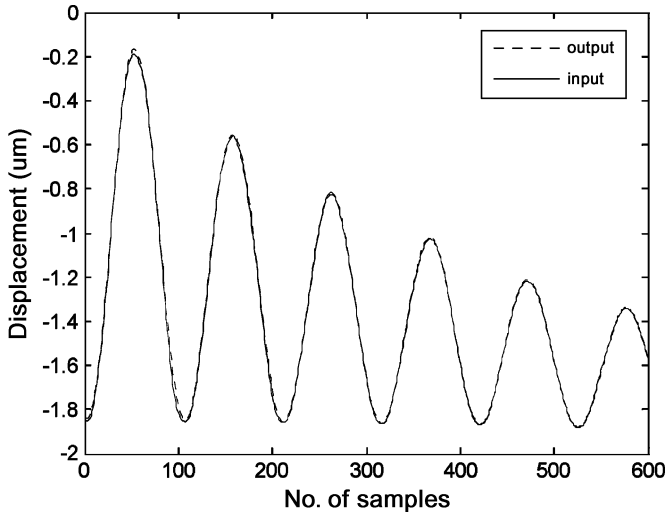

Fig. 12. Performance of the signal compensation.

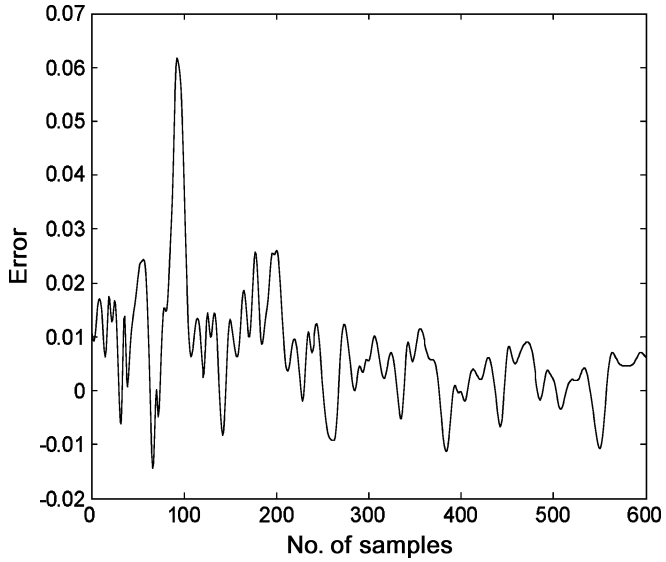

Fig. 13. Error of the signal compensation.

a direct inverse model controller to cancel the oscillation or vibration caused by the hysteresis. The corresponding input and output of the system is shown in Fig. 12. Moreover, the corresponding signal compensation error is illustrated in Fig. 13. It is seen that the maximum error is 0.0617. The result shows that the maximum error occurs at the maximum input extremum and the error is much less at the other input points. Clearly, the inverse hysteresis model can suppress the influence of hysteresis and improve the signal tracking performance.

VI. Conclusion

In order to adapt to the change of the operating condition and the variation of environment, a neural network is probably one of useful alternatives. As neural networks usually cannot directly be used for the approximation of the systems with multivalued mapping such as hystersis, a hysteretic operator is proposed to extract the movement tendency of hysteresis. Then, an expanded input space containing the proposed hysteretic operator is constructed to transform the multivalued mapping of hysteresis into a one-to-one mapping so that neural networks are capable of implementing identification for hysteresis. Similar to the method of modeling hystereis, an inverse hyteretic operator is also proposed to construct an inverse hysteresis model. Then, the inverse hysteresis model is used as a compensator in cascade with the real piezoelectric actuator to improve the performance of signal tracking. The experimental results and comparison with the well-known KP model have illustrated the potential of the proposed modeling technique.

Acknowledgment

The authors would like to thank the anonymous reviewers for their valuable comments.

References

[1] G. Tao and P. V. Kolotovic, "Adaptive control of plants with unknown hysteresis," *IEEE Trans. Autom. Control*, vol. 40, no. 2, pp. 200–212, Feb. 1995.

[2] I. D. Mayergoyz, *Mathematical Models of Hysteresis*. New York: Springer-Verlag, 1991.

[3] P. Ge and M. Jouaneh, "Generalized Preisach model for hysteresis nonlinearity of piezoceramic actuator," *Precision Eng.*, vol. 20, pp. 99–111, 1997.

[4] M. A. Krasnoskl'skii and A. V. Pokrovskii, *System with Hysteresis*. New York: Springer-Verlag, 1989.

[5] W. T. Ang *et al.*, "Modeling rate-dependent hysteresis in piezoelectric actuators," in *Proc. IEEE/RSJ Int. Conf. Intell. Roboot Syst.*, Oct. 2003, pp. 27–31.

[6] Y. K. Wen, "Method for random vibration of hysteretic systems," *J. Eng. Mech.*, vol. 102, pp. 249–263, 1976.

[7] A. A. Adly and S. K. Abd-El-Hafiz, "Using neural networks in the identification of Preisach-type hysteresis models," *IEEE Trans. Magn.*, vol. 34, no. 3, pp. 629–635, May 1998.

[8] C. Serpico and C. Visone, "Magnetic hyteresis modeling via feed-forward neural networks," *IEEE Trans. Magn.*, vol. 34, no. 3, pp. 623–628, May 1998.

[9] L. Chuntao and T. Yonghong, "A neural networks model for hysteresis nonlinearity," *Sens. Actuators, Phys. A*, vol. 112, pp. 49–54, 2004.

[10] G. V. Webb and D. C. Lagoudas, "Hysteresis modeling of SMA actuators for control application," *J. Int. Mater. Syst. Struct.*, vol. 9, pp. 432–448, 1998.

[11] J.-D. Wei and C.-T. Sun, "Constructing hysteretic memory in neural networks," *IEEE Trans. Syst., Man Cybern. B: Cybern.*, vol. 30, no. 4, pp. 601–609, Apr. 2000.

[12] M. J. D. Powell, "Restart procedures for the conjugate gradient method," *Math. Program.*, vol. 12, pp. 241–254, 1977.